Supplementary Information for

Persistent heavy winter nitrate pollution driven by increased photochemical oxidants in northern China

Xiao Fu [1], Tao Wang [1, *], Jian Gao [2], Peng Wang [1], Yiming Liu[1], Shuxiao Wang [3], Bin Zhao [3,4] and Likun Xue [5]

[1]Department of Civil and Environmental Engineering, Hong Kong Polytechnic University, Hong Kong 99907, China

[2]State Key Laboratory of Environmental Criteria and Risk Assessment, Chinese Research Academy of Environmental Sciences, Beijing 10084, China

[3]School of Environment, and State Key Joint Laboratory of Environment Simulation and Pollution Control, Tsinghua University, Beijing 100084, China

[4] Atmospheric Sciences and Global Change Division, Pacific Northwest National Laboratory, Richland, WA 99352, USA

[5]Environment Research Institute, Shandong University, Qingdao 266000, Shandong, China

Corresponding to: Tao Wang

Email: tao.wang@polyu.edu.hk

Telephone: +852-27666059

Number of pages: 14

Number of figures: 12

Number of tables: 4

1. Model Configuration

CMAQ version 5.1 with the SAPRC07tic gas mechanism and AERO6i aerosol mechanism was used in this study. The state-of-the-art N_2O_5 heterogeneous chemistry and HONO chemistry have been incorporated. Firstly, we have updated the calculation of heterogeneous uptake coefficient of N_2O_5 (γ_{N2O5}) on aerosols and the $ClNO_2$ yield (Φ_{ClNO2}) based on a new observation-based empirical parameterization, shown as equation [1] and [2].

$$\gamma_{N_2O_5} = \frac{4}{c}\frac{V_a}{S_a}K_H \times 3.0\times10^4 \times [H_2O(l)]\left(1 - \frac{1}{\left(0.033\times\frac{[H_2O(l)]}{[NO_3^-]}\right) + 1 + \left(3.4\times\frac{[Cl^-]}{[NO_3^-]}\right)}\right) \quad [1]$$

$$\Phi_{ClNO2} = \frac{[Cl^-]}{[H_2O]/105+[Cl^-]} \quad [2]$$

Where c is the mean molecular speed of N_2O_5; V_a/S_a is the particle volume to surface area ratio; K_H is the Henry's law coefficient. Detailed method and data to derive this parameterization can be found in Yu et al. [1] Secondly, comprehensive HONO sources have been considered, including HONO emissions from vehicles, gas-phase reaction of NO and OH, RH-dependent and light-enhancing effects on heterogeneous reactions, photolysis of particulate nitrate in the atmosphere, and photolysis of HNO_3 and nitrate deposited on surfaces [2]. Here, we updated the estimation for the photolysis rates of deposited nitrate (J_{DNO3})[3], as below.

$$J_{DNO3} = \frac{\frac{8.5\times10^{-4}}{2.5\times10^7 \times D_{HNO_3}} ln\left(1 + 2.5\times10^7 D_{HNO_3}\right) + 3.0\times10^{-6}}{7\times10^{-7}} \times J_{HNO3\text{-}CMAQ} \quad [3]$$

Where D_{HNO_3} is the deposited nitrate, and $J_{HNO3\text{-}CMAQ}$ is the photolysis rate of gaseous HNO_3 calculated online in CMAQ. Additionally, the uptake of HO_2 on the aerosol surface has been also incorporated into CMAQ [4, 5]. The online photolysis module in CMAQ is used to allow the calculation of actinic fluxes and photolysis rates based on the changes in particle concentrations.

Two nesting domains were used with their horizontal resolutions being 36 and 12km, respectively, and the land area in the innermost domain covers the NCP region (Fig. S2). These domains are based on a Lambert projection with two true latitudes of 25° N and 40° N. The meteorological field was generated by the Weather Research and Forecasting Model (WRF) version 4.0, whose physical options are same as Fu et al. [6] Data assimilation has been performed using the NCEP Automated Data Processing (ADP) Upper and Surface Air Observational Weather Data (ds351.0 and ds461.0).

The Chinese anthropogenic emission data for 2010 and 2015 were from Zhao et al. [7], which developed the emission inventory based on a bottom-up method with detailed Chinese local data. The 2017 anthropogenic emission data was generated by updating the 2015 data based on the ratio of 2017 emission to 2015 emission for China reported in Zheng et al. [8] In order to better represent vertical distribution of emissions, the emission heights of large industrial sources (e.g. power plants, cement plants, and iron and steel plants) were identified through obtaining the heights of stacks and calculating the plume rising heights under different weather conditions.

2. Model Evaluation

The observation data from the National Climatic Data Center (NCDC) was used to evaluate the reliability of the meteorological prediction. Table S1 summarizes the statistical performance for 10-m wind speed (WS10), 10-m wind direction (WD10), 2-m temperature (T2) and 2-m humidity (H2), and the results indicate the Weather Research and Forecasting Model (WRF) used in this study generally well reproduced these key surface meteorological parameters. Measurements of mixing height are scarce in China, and we cannot obtain the observation data for our study period (1-31 Dec. 2017). However, several previous studies[9, 10] have indicated that the WRF model can generally reproduce the variation of observed mixing heights during winter in the NCP region. In the present study, the WRF simulated monthly average daily maximum mixing height was ~1025m (with day-to-day maximum mixing height ranging from ~1600m to ~600m) during 1-31 Dec. 2017, which are in similar range of previously winter observations[9-12] in the NCP region, and the model well simulated the negative correlation between the mixing height and $PM_{2.5}$ concentrations (Fig. S3).

We evaluated the model performance for fine particle nitrate based on the daily average observations at 28 sites in the North China Plain (Fig. 1c) during 1-31 December, 2017. The revised CMAQ model can well capture the observed spatial and temporal variability of nitrate (Fig. 1c-e). The normalized mean bias (NMB) and correlation coefficient can reach 0.2% and 0.76, respectively. The model can generally reproduce the increasing NO_3^- concentrations with aggravating pollution (Fig. 1f), with an overestimation of 0.68 $\mu g/m^3$ (10.4%) under clean conditions (daily $PM_{2.5} < 75 \mu g/m^3$) and an underestimation of 3.61 $\mu g/m^3$ (7.9%) under heavily polluted conditions (daily $PM_{2.5} > 150 \mu g/m^3$). The model can also reproduce the increasing trend of NO_3^- percentage in $PM_{2.5}$ with aggravating pollution, although the simulated percentages are a

little higher than the observations due to the underestimation of OC and $PM_{2.5}$. We evaluated the model performance for O_3, NO_2 and $PM_{2.5}$ based on the hourly observations at 614 official monitoring sites in the NCP region from the China Ministry of Ecology and Environment (MEE) (Fig. S2). As shown in Table S2, The NMBs of O_3, NO_2 and $PM_{2.5}$ predictions are 12.8%, 4.9% and -2.5%, respectively, and the correlation coefficients (R) are all above 0.55, which are reasonably acceptable. The model can well capture the diurnal profiles and day-to-day variations of O_3, NO_2 and $PM_{2.5}$ (Fig.S4). Additionally, we compared the simulations of OH, HO_2, and their precursors (e.g. HONO, HCHO and H_2O_2) with field observations reported in the NCP region (Table S3). OH and HO_2 observations in China are limited, especially in winter. Tan et al. [13] reported average OH and HO_2 levels at noon time to be 2.36×10^6 cm^{-3} and 0.52×10^8 cm^{-3} in Beijing during January to March, 2016, which were much higher than several observations in the foreign countries. Our model can reproduce the high OH and HO_2 levels well. Meanwhile, the simulations also agree well with the surface observations of HONO, HCHO and H_2O_2 reported in the NCP region [14-19]. The model simulated vertical HONO profile (Fig S7b) compared reasonably well with previously observed one in Beijing[20].

Tables and Figures

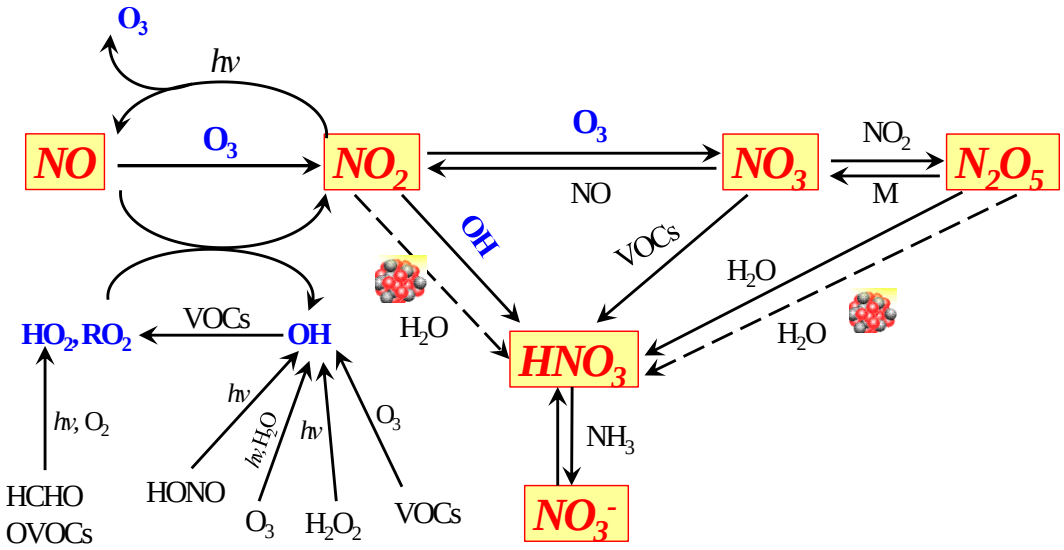

Figure S1 A schematic picture of complex reactions involving photochemical oxidants and nitrogen species.

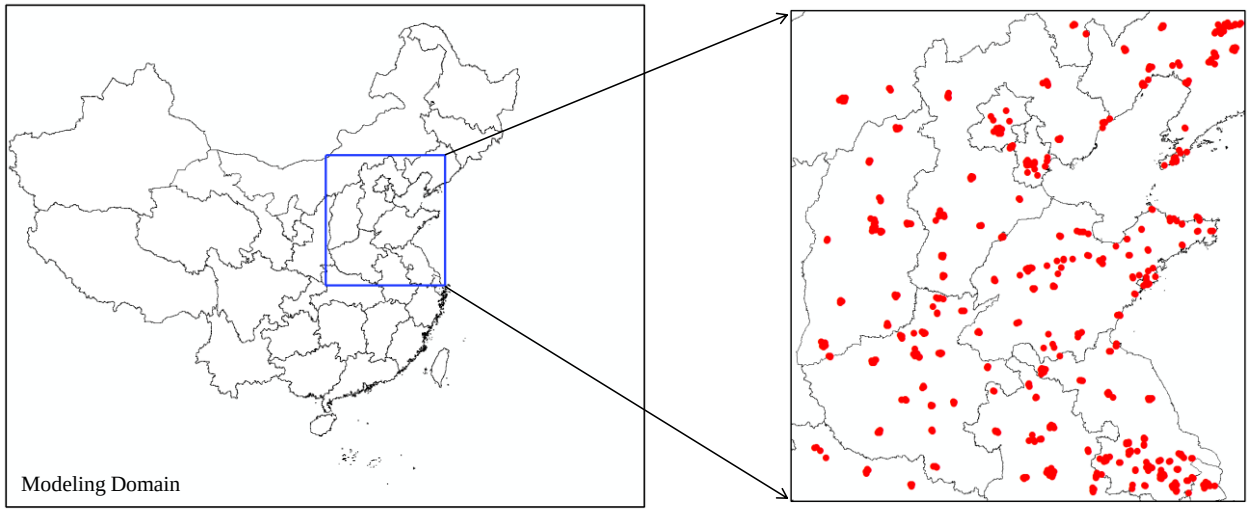

Figure S2 Model domains. Red dots represent official monitoring sites in the NCP region from the China Ministry of Ecology and Environment (MEE).

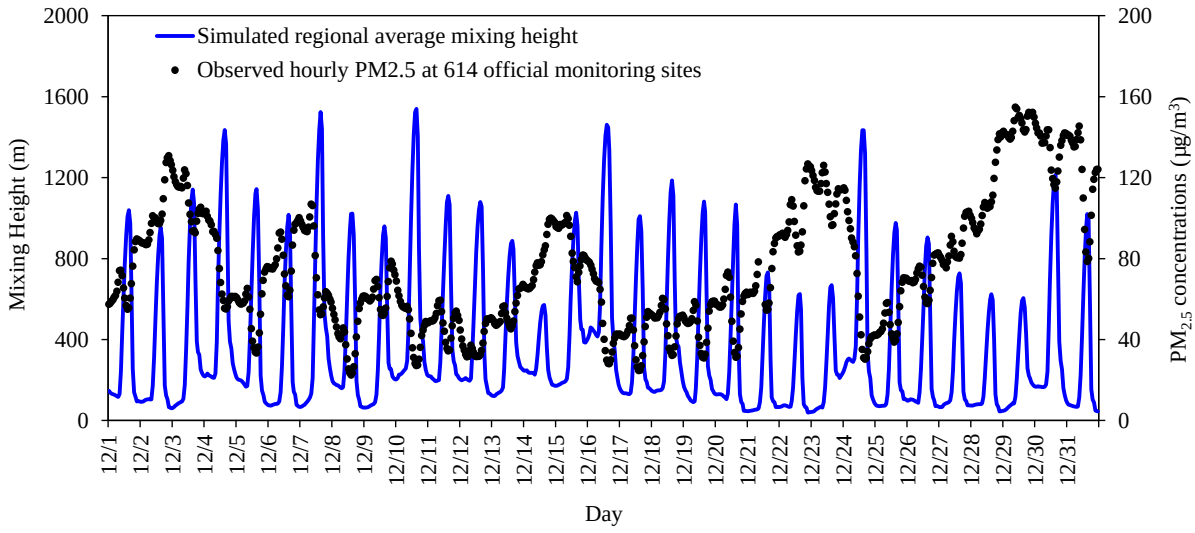

Figure S3 Simulated average hourly mixing height in the NCP region during 1-31 Dec. 2017 (blue line) and observed average hourly $PM_{2.5}$ concentrations at 614 official monitoring sites in the NCP region (black dots).

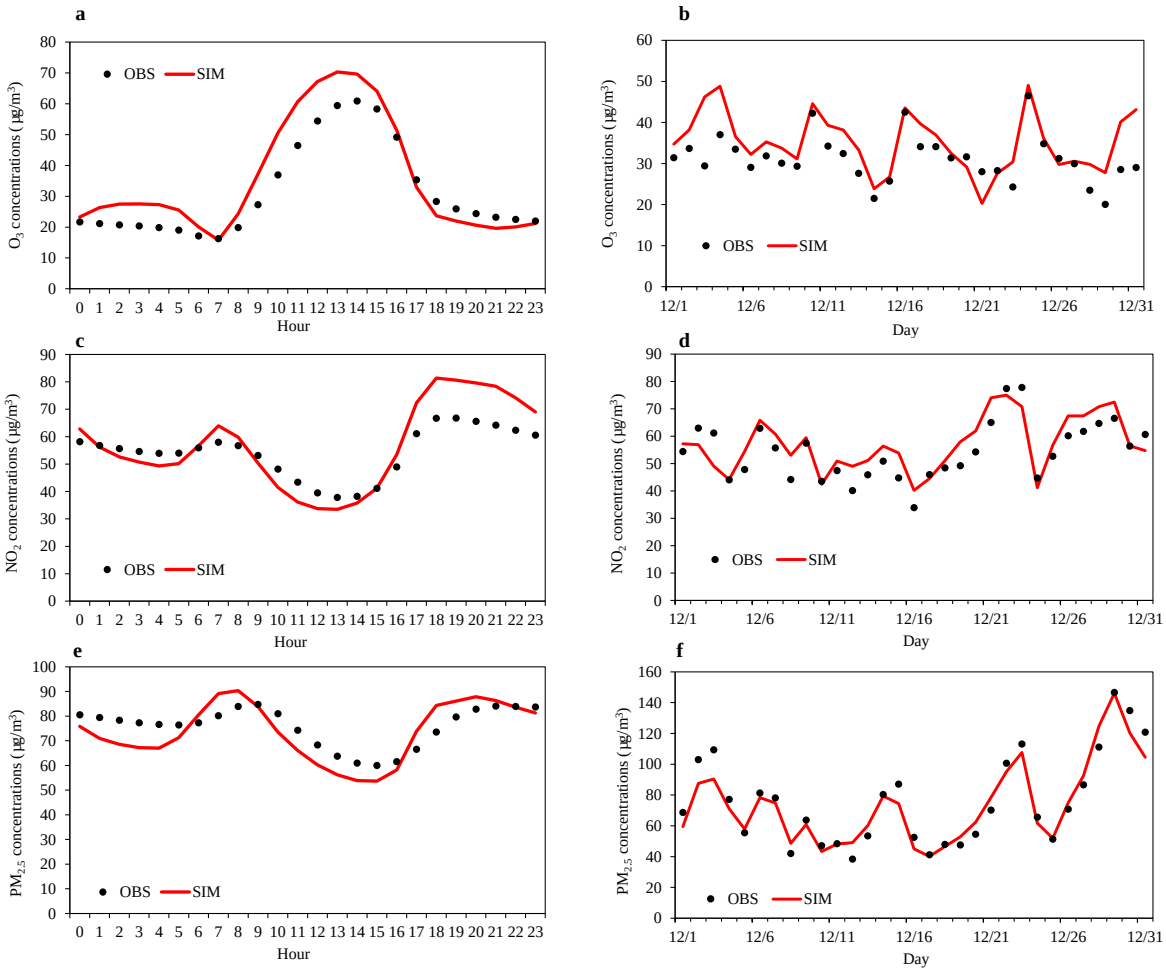

Figure S4 Simulated and observed diurnal profile and day-to-day variations of **(a-b)** O_3, **(c-d)** NO_2 and **(e-f)** $PM_{2.5}$ at official monitoring sites in the NCP region.

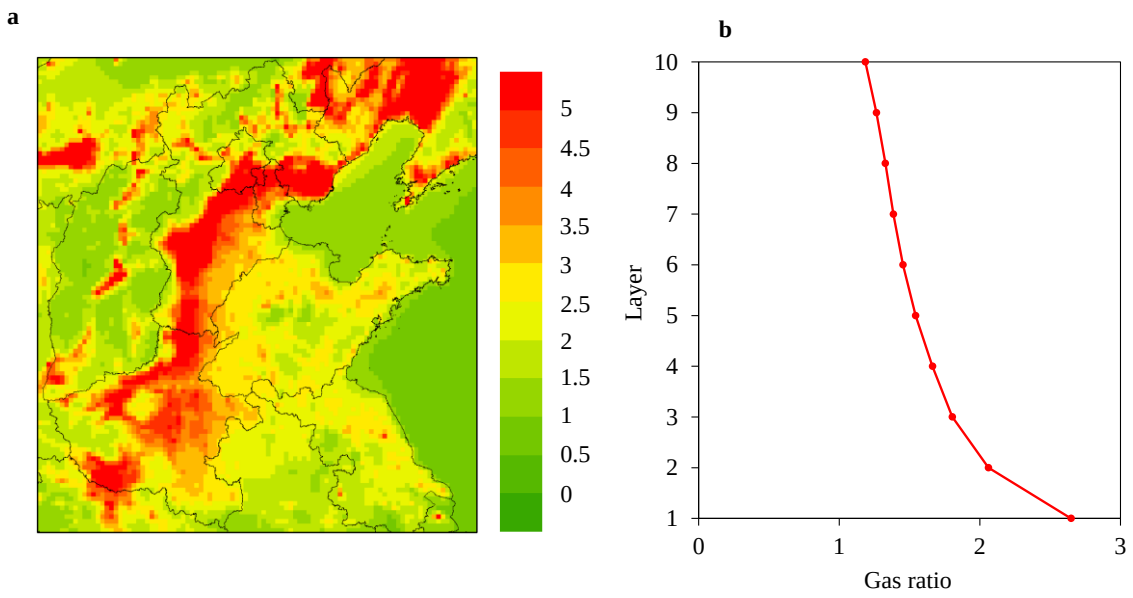

Figure S5 (**a**) Surface spatial and (**b**) vertical distribution of gas ratio (GR= $\frac{([NH_3]+[NH_4^+])-2\times[SO_4^{2-}]}{[NO_3^-]+[HNO_3]}$). GR>1 indicates NH_3-rich conditions, 0<GR<1 indicates NH_3-neutral conditions, and GR<0 indicates NH_3-poor conditions.

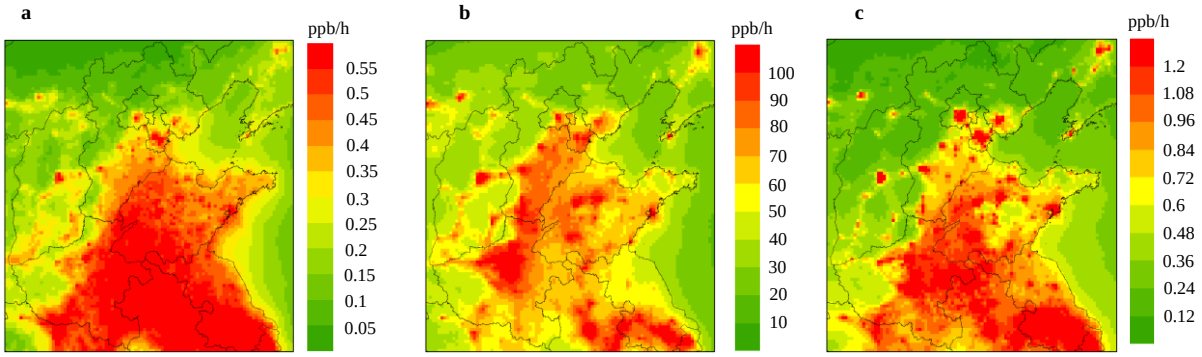

Figure S6 Spatial distributions of monthly average production rates at the surface layer for (**a**) HNO_3, (**b**) O_3, and (**c**) OH

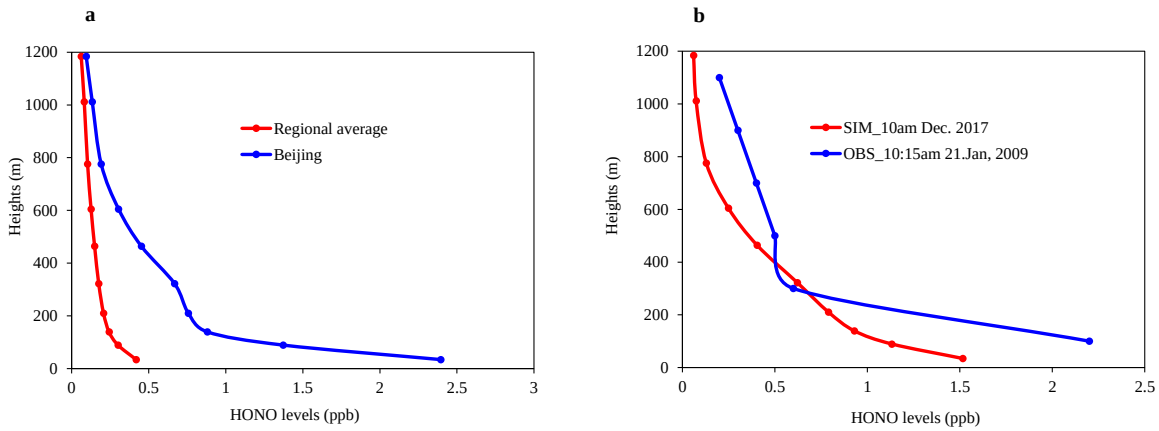

Figure S7 (a) Vertical distributions of the simulated average HONO levels in the NCP region and Beijing site (39.98° N, 116.38° E). **(b)** Vertical distributions of simulated (10:00am, 1-31 Dec. 2017) and observed (10:15am of 21 January 2009) at Beijing site.

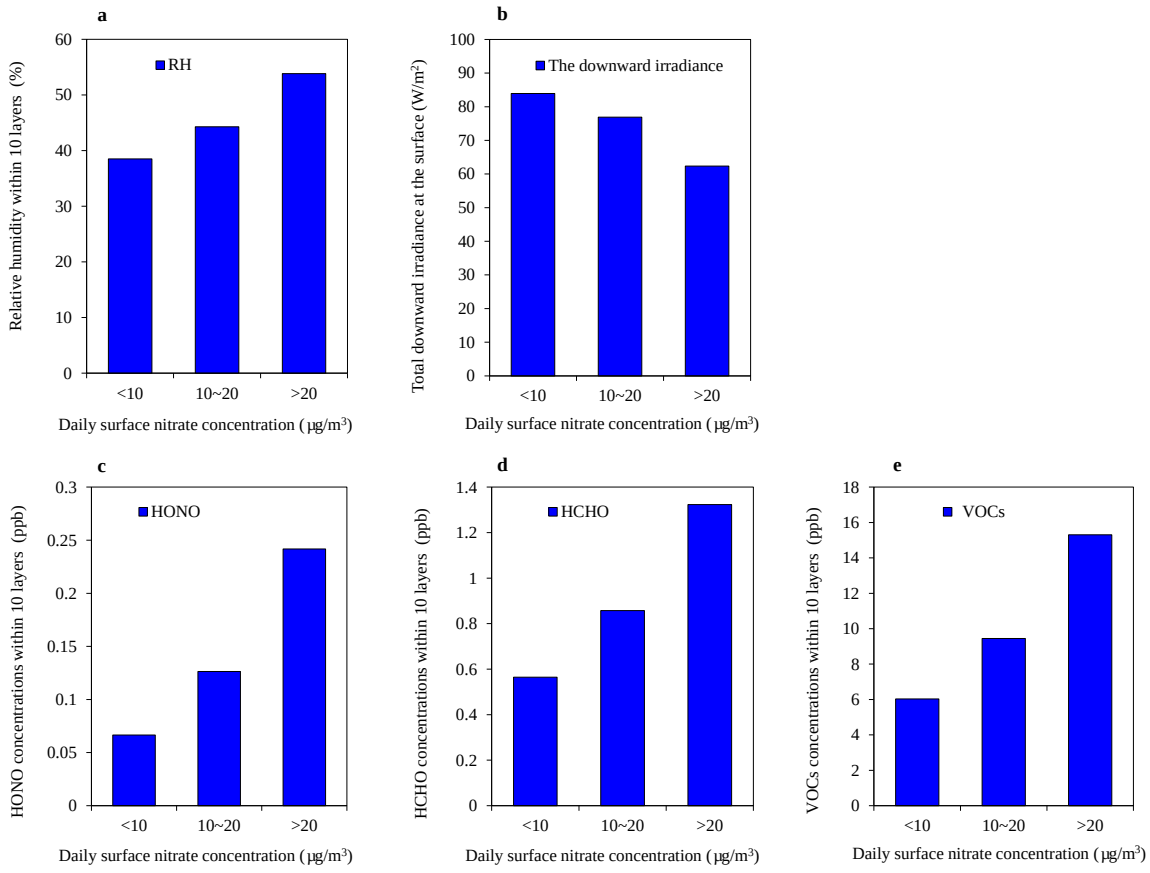

Figure S8 Variations of (**a**) relatively humidity, (**b**) the total downward irradiance at the surface, (**c**) HONO concentrations, (**d**) HCHO mixing ratios, and (**e**) VOCs mixing ratios, under different nitrate pollution levels. Three nitrate pollution levels are divided based on simulated daily average surface nitrate concentrations over the NCP region, with the concentration ranges of <10 μg/m^3, 10–20 μg/m^3, and > 20 μg/m^3.

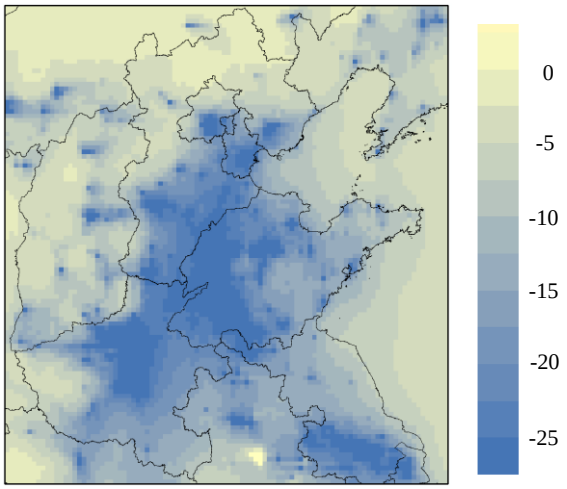

Figure S9 Changes in the simulated surface NO_X mixing ratios (ppb) due to emissions reductions during 2010-2017 (difference between the simulation 2017Emis and 2010Emis).

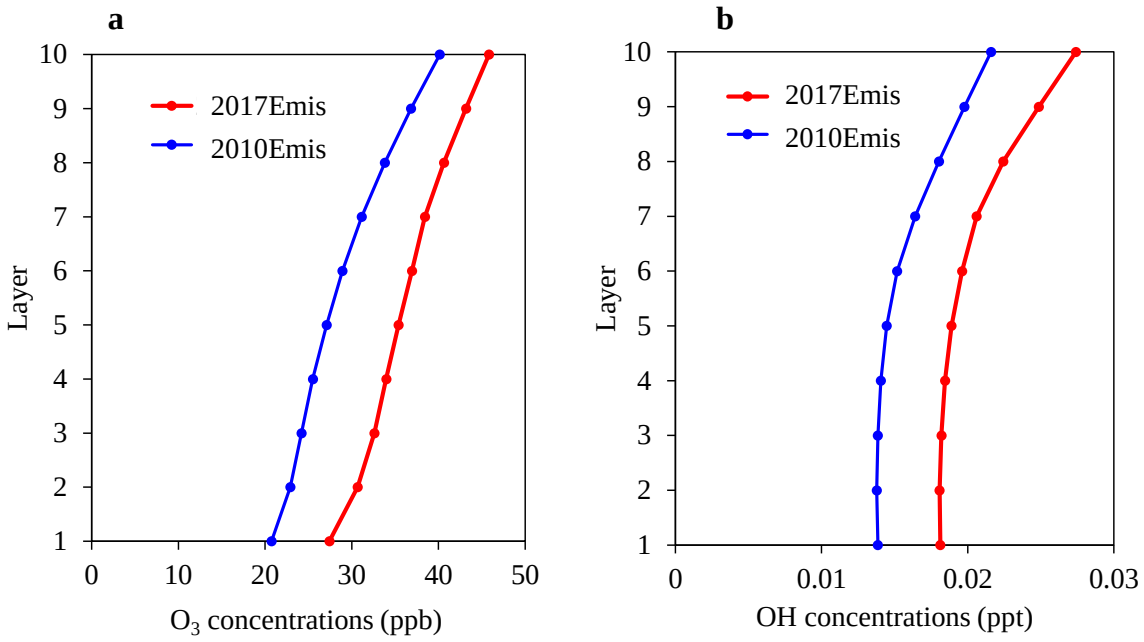

Figure S10 Oxidants changes over the NCP region from the simulations "2017Emis" and "2010Emis". (**a**) Vertical profile for average O_3 mixing ratios. (**b**) Vertical profile for average OH mixing ratios.

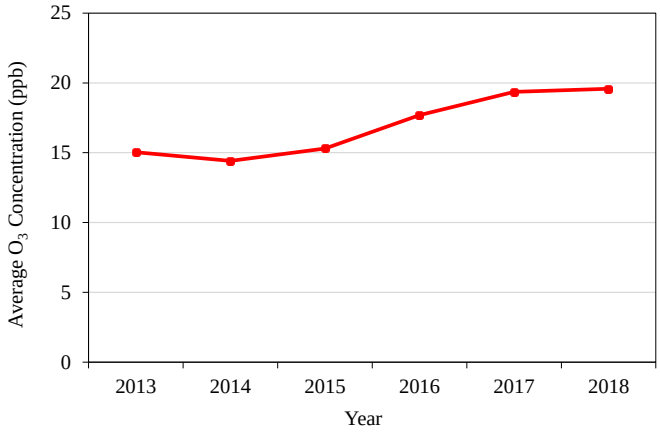

Figure S11 Annual variations of observed average O_3 mixing ratios in winter at the monitoring sites from the China Ministry of Ecology and Environment (MEE) from 2013 to 2018.

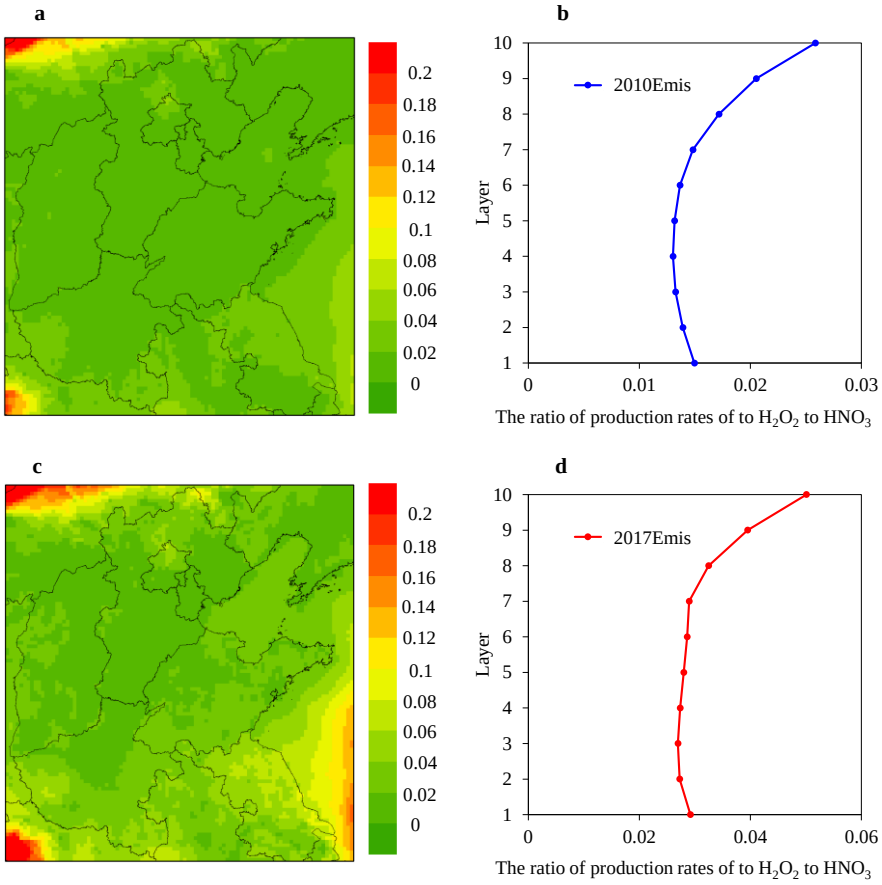

Figure S12 Simulated surface and vertical ratios of production rates of H_2O_2 to HNO_3 ($P_{H_2O_2}/P_{HNO_3}$) for the simulation "2010Emis" (**a-b**) and "2017Emis" (**c-d**). According to Zhang et al. [21], $P_{H_2O_2}/P_{HNO_3}$ of <0.06, 0.06–0.2, and >0.2 correspond to VOC-limited, transition, and NOx-limited conditions, respectively.

Table S1 Model performance statistics for meteorological variables in the innermost domain covering the NCP region

Variable	T2 (°C)	H2 (g/kg)	WS10 (m/s)	WD10 (°)
Mean OBS	4.0	4.0	2.7	241.1
Mean SIM	4.3	3.9	2.9	237.3
Bias	0.3	-0.1	0.2	-3.8
NMB (%)	9.3	-2.0	7.8	
NME (%)	35.4	14.7	44.4	

Table S2 Model performance for O_3, $PM_{2.5}$ and NO_2 at 614 monitoring sites in the NCP region

	OBS (μg/m^3)	SIM (μg/m^3)	Bias (μg/m^3)	NMB	R
O_3	31.3	35.3	4.0	12.8%	0.56
$PM_{2.5}$	75.7	73.8	-1.9	-2.5%	0.65
NO_2	54.3	57	2.7	4.9%	0.58

Table S3 Comparisons between simulated and observed OH, HO_2, HONO, H_2O_2, and HCHO over the NCP region from previous studies

Species	Location	Obs. period	Obs. average	Sim. average	Reference
OH (10^6 cm^{-3})	Huairou_Beijing	Jan-Mar, 2016	2.36 (noontime, polluted)	2.3 (noontime)	Tan et al. [13]
HO_2 (10^8 cm^{-3})	Huairou_Beijing	Jan-Mar, 2016	0.52 (noontime, polluted)	0.49 (noontime)	Tan et al. [13]
HONO (ppb)	ICCAS_Beijing	Dec, 2014	1.34	2.40	Tong et al. [16]
	CEE_Beijing	Jan, 2016	1.05	2.40	Wang et al. [17]
	EPA_Beijing	Feb-March, 2015	1.99	2.40	Zhang et al. [19]
	Jinan_Shandong	Dec-Feb, 2016	1.75	1.92	Li et al. [14]
H_2O_2 (ppb)	Beijing	Jan, 2016	0.25	0.34	Ye et al. [18]
	Wangdu_Hebei	Dec, 2017	0.23	0.32	Ye et al. [18]
HCHO (ppb)	Beijing	Dec, 2014	4.20	5.97	Song et al. [15]

Table S4 Scenario design for model simulations

Simulations	Emissions	Purpose
2017Emis	emissions in 2017	investigate the role of photochemical oxidants in the formation and aggravation of winter NO_3^- pollution
2010Emis	emissions in 2010	examine the response of NO_3^- concentrations to emissions reduction during 2010-2017 and its driving factors
2017Emis-30%VOC	2017Emis + an additional 30% VOC emission reduction	quantify the response of NO_3^- concentrations if VOC emissions had been simultaneously reduced by 30% during 2010-2017

References

1. Yu, C.; Wang, Z.; Xia, M.; Fu, X.; Wang, W.; Tham, Y. J.; Chen, T.; Zheng, P.; Li, H.; Shan, Y.; Wang, X.; Xue, L.; Zhou, Y.; Yue, D.; Ou, Y.; Gao, J.; Lu, K.; Brown, S. S.; Zhang, Y.; Wang, T., Heterogeneous N2O5 reactions on atmospheric aerosols at four Chinese sites: Improving model representation of uptake parameters. *Atmos. Chem. Phys. Discuss.* **2019**.
2. Fu, X.; Wang, T.; Zhang, L.; Li, Q.; Wang, Z.; Xia, M.; Yun, H.; Wang, W.; Yu, C.; Yue, D.; Zhou, Y.; Zheng, J.; Han, R., The significant contribution of HONO to secondary pollutants during a severe winter pollution event in southern China. *Atmospheric Chemistry and Physics* **2019,** *19*, (1), 1-14.
3. Ye, C.; Gao, H.; Zhang, N.; Zhou, X., Photolysis of Nitric Acid and Nitrate on Natural and Artificial Surfaces. *Environmental Science & Technology* **2016,** *50*, (7), 3530-3536.
4. Jacob, D. J., Heterogeneous chemistry and tropospheric ozone. *Atmospheric Environment* **2000,** *34*, (12-14), 2131-2159.
5. Li, K.; Jacob, D. J.; Liao, H.; Shen, L.; Zhang, Q.; Bates, K. H., Anthropogenic drivers of 2013-2017 trends in summer surface ozone in China. *Proceedings of the National Academy of Sciences of the United States of America* **2019,** *116*, (2), 422-427.
6. Fu, X.; Wang, S.; Chang, X.; Cai, S.; Xing, J.; Hao, J., Modeling analysis of secondary inorganic aerosols over China: pollution characteristics, and meteorological and dust impacts. *Scientific Reports* **2016,** *6*.
7. Zhao, B.; Zheng, H.; Wang, S.; Smith, K. R.; Lu, X.; Aunan, K.; Gu, Y.; Wang, Y.; Ding, D.; Xing, J.; Fu, X.; Yang, X.; Liou, K.-N.; Hao, J., Change in household fuels dominates the decrease in PM2.5 exposure and premature mortality in China in 2005-2015. *Proceedings of the National Academy of Sciences of the United States of America* **2018,** *115*, (49), 12401-12406.
8. Zheng, B.; Tong, D.; Li, M.; Liu, F.; Hong, C.; Geng, G.; Li, H.; Li, X.; Peng, L.; Qi, J.; Yan, L.; Zhang, Y.; Zhao, H.; Zheng, Y.; He, K.; Zhang, Q., Trends in China's anthropogenic emissions since 2010 as the consequence of clean air actions. *Atmospheric Chemistry and Physics* **2018,** *18*, (19), 14095-14111.
9. He, H.; Tie, X.; Zhang, Q.; Liu, X.; Gao, Q.; Li, X.; Gao, Y., MU Analysis of the causes of heavy aerosol pollution in Beijing, China: A case study with the WRF-Chem model. *Particuology* **2015,** *20*, 32-40.
10. Lu, Z.; Han, Y.; Xia, J.; Zhao, T., Modeling study on boundary layer height in pollution weather by WRF with different boundary layer schemes. *China Environmental Science* **2018,** *38*, (3), 822-829.
11. Su, T.; Li, Z.; Kahn, R., Relationships between the planetary boundary layer height and surface pollutants derived from lidar observations over China: regional pattern and influencing factors. *Atmospheric Chemistry and Physics* **2018,** *18*, (21), 15921-15935.
12. Wang, J.; Cai, X.; Song, Y., Daily Maximum Height of Atmospheric Boundary Layer in Beijing: Climatology and Environmental Meaning. *Climatic and Environmental Research* **2016,** *21*, (5), 525-532.
13. Tan, Z.; Rohrer, F.; Lu, K.; Ma, X.; Bohn, B.; Broch, S.; Dong, H.; Fuchs, H.; Gkatzelis, G. I.; Hofzumahaus, A.; Holland, F.; Li, X.; Liu, Y.; Liu, Y.; Novelli, A.; Shao, M.; Wang, H.; Wu, Y.; Zeng, L.; Hu, M.; Kiendler-Scharr, A.; Wahner, A.; Zhang, Y., Wintertime photochemistry in Beijing: observations of ROx radical concentrations in the North China Plain during the BEST-ONE campaign. *Atmospheric Chemistry and Physics* **2018,** *18*, (16), 12391-12411.

14. Li, D.; Xue, L.; Wen, L.; Wang, X.; Chen, T.; Mellouki, A.; Chen, J.; Wang, W., Characteristics and sources of nitrous acid in an urban atmosphere of northern China: Results from 1-yr continuous observations. *Atmospheric Environment* **2018,** *182*, 296-306.
15. Song, S. J.; Gao, M.; Xu, W. Q.; Sun, Y. L.; Worsnop, D. R.; Jayne, J. T.; Zhang, Y. Z.; Zhu, L.; Li, M.; Zhou, Z.; Cheng, C. L.; Lv, Y. B.; Wang, Y.; Peng, W.; Xu, X. B.; Lin, N.; Wang, Y. X.; Wang, S. X.; Munger, J. W.; Jacob, D. J.; McElroy, M. B., Possible heterogeneous chemistry of hydroxymethanesulfonate (HMS) in northern China winter haze. *Atmospheric Chemistry and Physics* **2019,** *19*, (2), 1357-1371.
16. Tong, S.; Hou, S.; Zhang, Y.; Chu, B.; Liu, Y.; He, H.; Zhao, P.; Ge, M., Exploring the nitrous acid (HONO) formation mechanism in winter Beijing: direct emissions and heterogeneous production in urban and suburban areas. *Faraday Discussions* **2016,** *189*, 213-230.
17. Wang, J.; Zhang, X.; Guo, J.; Wang, Z.; Zhang, M., Observation of nitrous acid (HONO) in Beijing, China: Seasonal variation, nocturnal formation and daytime budget. *Science of the Total Environment* **2017,** *587*, 350-359.
18. Ye, C.; Liu, P. F.; Ma, Z. B.; Xue, C. Y.; Zhang, C. L.; Zhang, Y. Y.; Liu, J. F.; Liu, C. T.; Sun, X.; Mu, Y. J., High H2O2 Concentrations Observed during Haze Periods during the Winter in Beijing: Importance of H2O2 Oxidation in Sulfate Formation. *Environmental Science & Technology Letters* **2018,** *5*, (12), 757-763.
19. Zhang, R.; Sun, X.; Shi, A.; Huang, Y.; Yan, J.; Nie, T.; Yan, X.; Li, X., Secondary inorganic aerosols formation during haze episodes at an urban site in Beijing, China. *Atmospheric Environment* **2018,** *177*, 275-282.
20. Hendrick, F.; Muller, J. F.; Clemer, K.; Wang, P.; De Maziere, M.; Fayt, C.; Gielen, C.; Hermans, C.; Ma, J. Z.; Pinardi, G.; Stavrakou, T.; Vlemmix, T.; Van Roozendael, M., Four years of ground-based MAX-DOAS observations of HONO and NO2 in the Beijing area. *Atmospheric Chemistry and Physics* **2014,** *14*, (2), 765-781.
21. Zhang, Y.; Wen, X. Y.; Wang, K.; Vijayaraghavan, K.; Jacobson, M. Z., Probing into regional O-3 and particulate matter pollution in the United States: 2. An examination of formation mechanisms through a process analysis technique and sensitivity study. *Journal of Geophysical Research-Atmospheres* **2009,** *114*.